Thermochimica Acta, 149 (1989) 205–213
Elsevier Science Publishers B.V., Amsterdam – Printed in The Netherlands

THE EFFECT OF THE SURFACE HYDROXYLS ON THE CHLORINATION KINETICS OF ALUMINA

I.S. PAP, G. MINK, I. BERTÓTI, B. ZELEI and T. SZÉKELY

Research Laboratory for Inorganic Chemistry of the Hungarian Academy of Sciences, P.O. Box 132, H-1502 Budapest (Hungary)

T. HAUTHAL, G. BLUMENTHAL and G. KRANZ

Central Institute of Inorganic Chemistry, Academy of Sciences of G.D.R., 1199 Adlershof, Rudower Chaussee, Berlin (G.D.R.)

(Received 16 December 1988)

ABSTRACT

The chlorination kinetics of alumina samples containing various amounts of surface hydroxyls were studied by thermogravimetry. The phase composition and the specific surface area of the reacting solids were characterized by X-ray diffraction (XRD), IR and BET methods. At temperatures where the reaction rate was controlled by the chemical process the highest initial reaction rates were observed on the partially dehydroxylated samples prepared from gibbsite at 670 K. The high reactivity towards phosgene was attributed to the special role of the surface hydroxyls in the chlorination process. At high conversions, however, a significant decrease in the reaction rate was observed; this can be explained by the consumption of amorphous and transition alumina phases which leaves behind less reactive boehmite of much lower specific surface area.

INTRODUCTION

Chlorine metallurgy has been proposed as an alternative method for the processing of alumina-containing raw materials [1–4]. During the chlorination the actual surface structure and phase composition [5,6] as well as the surface hydroxyls [4,7] have a great influence on the reaction rate. The special effects of surface hydroxyls on the chlorination of kaolin [8] and on the dehydroxylation products of gibbsite [9] have recently been shown. Our aim is to compare the reactivity of alumina samples containing various amounts of surface hydroxyls. This paper reports a detailed kinetic investigation of the chlorination reactions of two partially dehydroxylated samples prepared from gibbsite and of a high purity γ-alumina with low OH coverage, using $COCl_2$ as chlorinating agent.

EXPERIMENTAL

Two alumina samples containing surface hydroxyls were prepared from gibbsite by calcining at 670 K (sample 1) and 820 K (sample 2) in a nitrogen flow for 30 min. The mass loss measured after the pretreatment and the physical characterization of the samples are given in Table 1. The phase compositions of the samples were determined using X-ray diffraction (XRD), and the initial specific surface areas were measured by oxygen physisorption at 77 K using the normal BET method. For comparison, the chlorination reaction of a high purity γ-alumina (Ketjen, The Netherlands) (sample 3) was also studied. Before the reactions this sample was preheated at 1120 K for 30 min in nitrogen to achieve a standard state with low residual OH content. According to the literature data [10] the surface OH coverage may be estimated as 3–5%.

Under the reaction conditions applied all the products are volatile, and so the reaction kinetics were followed by thermogravimetric measurements using a modified Mettler thermobalance [11]. Phosgene (purity, 99.9%) and nitrogen (purity, 99.99%) were used as chlorinating and inert carrier gases respectively. The solid residues obtained after the chlorination process were characterized by XRD, IR and BET methods.

RESULTS AND DISCUSSION

Isothermal TG measurements were carried out in the temperature range 550–820 K at partial pressure of phosgene of 10.1 kPa. The conversion (relative mass loss) vs. time curves for the samples prepared from gibbsite

TABLE 1

Characteristics of the samples used in the chlorination measurements

	Sample number		
	1	2	3
Starting material	Gibbsite	Gibbsite	γ-Alumina
Pretreating temperature (K) (N_2, 30 min)	670	820	1120
Mass loss (%) during the calcination	30	34	
Degree of dehydroxylation	0.86	0.97	
Surface area (m^2 g^{-1})	364	274	160
Phase composition (XRD)	Amorphous + boehmite + a small amount of χ-alumina	Amorphous + transition aluminas (γ and χ)	γ-Alumina

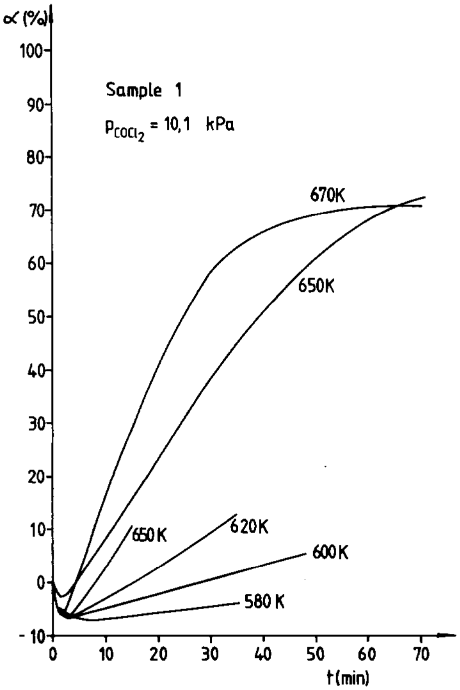

Fig. 1. Conversion vs. time curves for sample 1 prepared from gibbsite at 670 K.

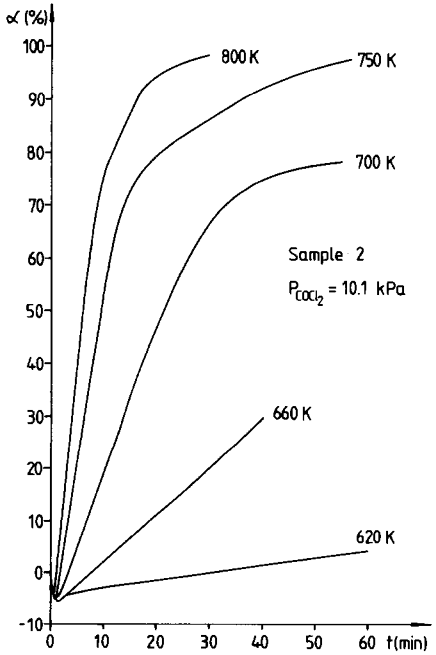

Fig. 2. Conversion vs. time curves for sample 2 prepared from gibbsite at 820 K.

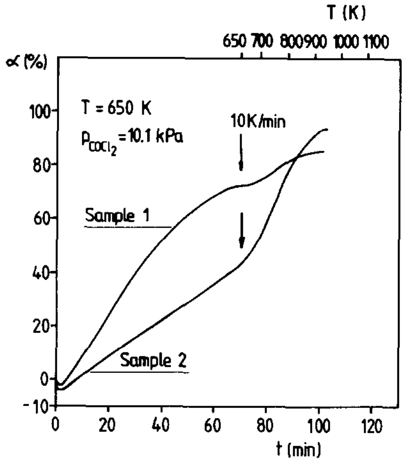

Fig. 3. Isothermal chlorination curves at 650 K, followed by an anisothermal treatment, also in $COCl_2$–N_2 flow.

are shown in Figs. 1 and 2. As with our previous results on the chlorination of γ-alumina [12], in each case the reaction starts with a fast mass gain which is attributed to the reaction of surface hydroxyls with phosgene, resulting in surface oxygen–chlorine exchange. This stage is followed by a continuous mass loss due to the volatilization of hydrogen chloride and aluminium chloride [9]. The reaction rate is determined as the slope of the initial linear part of the TG curves related to the initial surface area.

Figure 3 shows two thermogravimetric curves, where the isothermal chlorination step is followed by anisothermal heating, also in a flow of $COCl_2$ and nitrogen. As can be seen, during the reaction at 650 K a higher reaction rate is observed for sample 1 than for sample 2. (The reaction rates related to the initial surface area are 0.045 and 0.028 mg m^{-2} min^{-1} for samples 1 and 2 respectively.) Thus in accordance with our previous results [9] sample 1, which is partially dehydrated at 670 K, is more reactive towards phosgene in the initial part of the reaction. As the chlorination seems to terminate above a conversion value of 70% on sample 1, the system is then turned to anisothermal mode with a linear heating rate of 10 K min^{-1}. The heating results in a moderate increase in the conversion up to about 87%. For sample 2 the conversion achieved at the end of the anisothermal heating is about 93%. This means that sample 2 is more reactive at the final stage of chlorination than sample 1.

For comparison, the temperature dependences of the initial rates for the partially dehydroxylated samples (samples 1 and 2) and for the γ-alumina with low surface OH content (sample 3) are shown in Fig. 4. The Arrhenius representation of the reaction rates related to the initial surface area is shown in Fig. 5, and the calculated activation energies are given in Table 2.

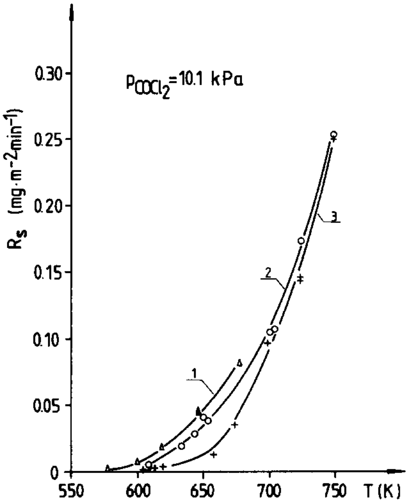

Fig. 4. The temperature dependence of the initial reaction rates: 1, sample 1; 2, sample 2; 3, sample 3.

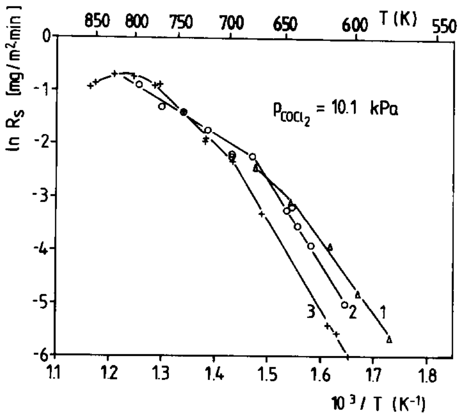

Fig. 5. The Arrhenius representation of the initial reaction rates: 1, sample 1; 2, sample 2; 3, sample 3.

TABLE 2

Apparent activation energies

Sample number	E (kJ mol^{-1})
1	124 (580–650 K)
2	121 (600–680 K)
	63 (680–820 K)
3	134 (600–700 K)

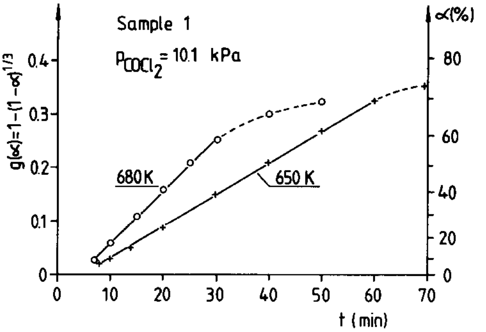

Fig. 6. g(α) vs. t curves for sample 1.

As can be seen in Fig. 5, below 650 K, i.e. at temperatures where the reaction is controlled by the chemical process, the chlorination rates are much higher in the hydroxyl-containing samples. The reactivity towards phosgene is attributed to the special role of the surface OH groups in the chlorination process according to their double function [9]: as Brönsted acids they are effective phosgene acceptors, and hydrogen chloride is produced simultaneously, which may also accelerate the chlorination by phosgene [13]. The values of the apparent activation energies are very similar for all the samples (Table 2). Above 650 K the slopes of the Arrhenius plots decrease. For sample 2 the apparent activation energy is about one-half of that calculated in the chemically controlled range. This suggests that at about 700 K the reaction changes to a pore-diffusion controlled reaction. There is no significant difference in the chlorination rates at these temperatures, as the reaction rates are determined primarily by transport processes for all the samples.

To describe the fractional order with respect to the solid, various kinetic models [14] were tested for the chlorination of samples 1 and 2. In both cases the contracting sphere model ($g(\alpha) = 1 - (1 - \alpha)^{1/3}$) proved to be the most satisfactory, giving the best fit in the conversion range $0.10 \leqslant \alpha \leqslant 0.70$ (correlation coefficients, $\geqslant 0.999$). The g(α) vs. t plots, all referring to the transport-controlled region, are shown in Figs. 6 and 7. In the case of sample 1 after a conversion of 70% is achieved, an ultimate cessation of the reactivity is observed. For sample 2 the slopes of the g(α) vs. t curves also decrease at high conversions, but in this case no termination occurs.

During the chlorination of γ-alumina with low OH content (sample 3) the isothermal TG curves can be described by the equation of the contracting cylinder model ($g(\alpha) = 1 - (1 - \alpha)^{1/2}$) up to a conversion of about 95%, i.e. the reactivity of this sample does not decrease during the chlorination. Figure 8 shows the g(α) vs. t representation for the chlorination of γ-alumina (sample 3) at 800 K and at a partial pressure of 10.1 kPa.

To interpret the formation of a relatively inactive residue which is produced during the chlorination of the partially dehydroxylated samples,

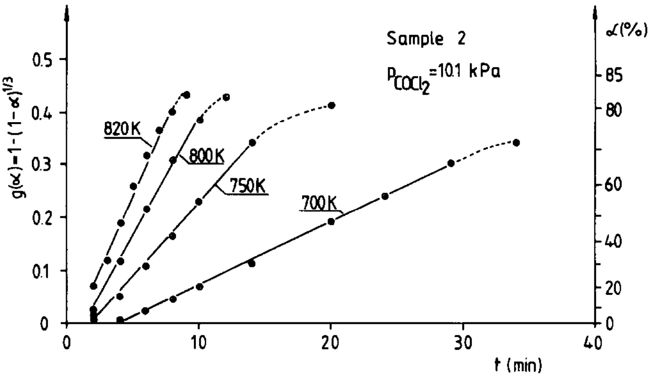

Fig. 7. g(α) vs. t curves for sample 2.

separate chlorination measurements were carried out at 670 K. The solid residues were analysed by XRD and IR methods, and the surface areas of the samples were determined using the BET method. The results are given in Table 3. By considering the data given in Tables 1 and 3 and the results of the TG measurements, the following conclusions can be drawn.

(i) The dehydroxylation of gibbsite at 670 K leads to boehmite and transition aluminas with high amorphous content and results in a very high surface area. This product shows a high activity in chlorination reactions. The boehmite phase seems to be inactive towards phosgene at this reaction temperature. In accordance with this observation Tsuchida et al. [5] reported a relatively low reactivity of the boehmite phase in the chlorination of hydrated aluminas. During the chlorination of sample 1 the amorphous component and the transition aluminas vigorously react with phosgene.

(ii) At the same time, part of the boehmite phase becomes more and more crystalline in the chlorinating atmosphere. This type of mineralizing effect of halogen-containing gases (in the present system HCl and $AlCl_3$) is well

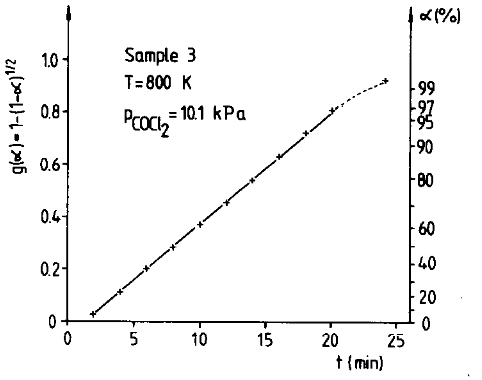

Fig. 8. g(α) vs. t curves for sample 3 at $T = 800$ K.

TABLE 3

The physical characteristics of the chlorinated residues of samples 1 and 2

	Sample number	
	1	2
Calcination temperature (K)	670	820
Surface area (m^2 g^{-1})	364	274
Chlorination temperature (K)	670	670
Conversion (%)	71	83
Phase composition (XRD)	Reduction in amorphous compounds Increase in boehmite	A moderate reduction in amorphous compounds Increase in transition aluminas (mostly γ-Al_2O_3)
Surface area (m^2 g^{-1})	17	155
Conversion (%)	68	71
Phase composition (IR)	Mostly boehmite Small amount of γ-alumina	Mostly γ-alumina

known from the literature [15,16]. During these processes all the amorphous and transition components are chlorinated, and the surface area drops to 17 m^2 g^{-1}. Thus the chlorination stops (see Figs. 1 and 3).

(iii) With increasing temperature further dehydroxylation of the well-crystallized boehmite component is resumed in an atmosphere of nitrogen or $COCl_2$. During these processes new active phases are produced and the chlorination by phosgene starts again (see Fig. 3).

(iv) The dehydroxylation of gibbsite at 820 K leads mainly to γ-alumina with a medium amount of amorphous components. This sample is also of remarkably high surface area. During the chlorination reactions a mineralizing effect occurs. The XRD measurements detect well-crystallized γ-alumina, a reduction in amorphous components and the formation of transition aluminas belonging to the δ-group (which are formed in the transition of γ-alumina to α-alumina). After a conversion of $\alpha = 84\%$ the residue still has a high surface area of 155 m^2 g^{-1}. Thus the chlorination does not terminate at about 70% as in sample 1 (see Fig. 3). However, above this conversion a remarkable decrease in the reactivity to chlorination, caused by the formation of δ-aluminas, is observed (see Fig. 2).

REFERENCES

1 R.A.J. Shelton, Trans. Indian Inst. Met., 30 (1977) 190.
2 J.G. Peacey and W.G. Davenport, J. Met., 26 (1977) 25.
3 A. Landsberg, Met. Trans. B, 6 (1975) 207.

4 G. Blumenthal, Zur Bedeutung der anorganischen Chlorierung: Chlorierung von Aluminium-Rohstoffen und Verbindungen, Dissertation B, Akad. D. Wiss. DDR, Berlin-Adlershof, 1987.
5 T. Tsuchida, T. Ishii, R. Furuichi and H. Haga, Thermochim. Acta, 34 (1979) 19.
6 R. He, M. Rohner and W. Richarz, Thermochim. Acta, 102 (1986) 349.
7 J. Basset, M.-V. Mathieu and M. Prettre, Rev. Chim. Miner., 5 (1968) 879.
8 G. Wegner, G. Blumenthal and T. Hauthal, G.D.R. Patent, 222 273 Al, 1983.
9 T. Hauthal, I.S. Pap, G. Blumenthal, I. Bertóti, G. Mink and T. Székely, Thermochim. Acta, 115 (1987) 269.
10 M. Zamora and A. Cordoba, J. Phys. Chem., 82 (1978) 584.
11 I. Bertóti, A. Tóth, T. Székely and I.S. Pap, Thermal Analysis, ICTA 80, Vol. 2, Birkhaeuser Verlag, Basel, 1980, p. 235.
12 I. Bertóti, A. Tóth, I.S. Pap and T. Székely, Thermochim. Acta, 44 (1981) 379.
13 G. Blumenthal, T. Hauthal and A. Radde, G.D.R. Patent, 206 980, 1982.
14 J.H. Sharp, G.W. Brindley and B.N. Achar, J. Am. Ceram. Soc., 49 (1966) 379.
15 D. Petzold, H. Hlawatschek, H. Konovalov, K. Herklotz and C. Hille, Freiberg Forschungsh. A, 653 (1981) 2163.
16 Z.D. Zickovic, N. Pacovic and M. Filipovic, Thermochim. Acta, 32 (1979) 181.